Visualization of quantum fluctuations by superposition of optimized nonorthogonal Slater determinants

Norikazu Tomita
Yamagata University, 1-4-12 Kojirakawa, Yamagata 990-8560, Japan
(Received 23 June 2008; revised manuscript received 23 December 2008; published 13 February 2009)

Electronic states in the one-dimensional (1D) doped Hubbard model are described by superposition of optimized nonorthogonal Slater determinants (S-dets). Analysis on the S-dets allows us to visualize quantum fluctuations. In the weak and intermediate interaction regimes, quantum fluctuations are described by translation and breathing motions of spin-charge coupled defects called polarons as well as spin-charge decoupled defects called holons and spinons. In the strong-interaction regime, on the other hand, spin and charge fluctuations are mostly separated as spinons and holons, especially in the lightly doped systems (δ=0.08). In the highly doped systems (δ=0.24), polarons also play an important role. Finally, it is shown that in the 1/3-filled systems, the concepts of holon, spinon, and polaron do not work anymore. The electronic structure is qualitatively described by mixtures of two different density waves having triple periodicity to the lattice. The domains of these different density waves make quantum fluctuations.

DOI: 10.1103/PhysRevB.79.075113 PACS number(s): 71.10.Fd, 71.15.−m

I. INTRODUCTION

Quantum fluctuations in low-dimensional electron systems have been one of the central issues in the condensed matters physics. A spin-charge separation is a good example showing unconventionality of elementary excitations in low dimensions. In the case of the one-dimensional (1D) Hubbard model, the wave function is exactly factorized into the spin and charge degrees of freedom in the strong-interaction limit.[1,2] On the other hand, in the weak-interaction limit, this model corresponds to a so-called Hückel model, and an electron or hole, which has both the spin and charge degrees of freedom, becomes a carrier. However, real materials do not lie in such extreme limits, and it is still controversial how the spin and charge behave in the realistic interaction regime. For example, two branches, corresponding to the spin and charge degrees of freedom, have been observed in the angle-resolved photoemission spectroscopy (ARPES) experiments on the 1D copper oxides.[3] However, at the same time, these experiments, as well as other ARPES results,[4,5] have suggested more complicated behaviors of elementary excitations. Specifically, broad peaks in the ARPES data suggest a significant spin-charge coupling in the 1D correlated electron systems.[6] So far, most of the theoretical and experimental researches have focused on separation of spin and charge degrees of freedom because of its unconventionality. However, in real materials, situations should be more complicated, and spin-charge coupling may play an important role. One of the purposes of the present research is to clarify the spin and charge behaviors in the 1D electron systems through the quantum fluctuations.

The spin-charge coupling (or decoupling) has also been attracting considerable attention in the quasi-two-dimensional (quasi-2D) high T_C cuprates. We have quite contrastive ideas on the mechanism of the high T_C superconductivity, based on the resonating valence bond[7] and spin bag,[8] as well as the perturbation approach from the weak-interaction limit.[9] The research on the spin-charge behaviors in the 1D electron systems is important because it would help us to understand the carriers in the high T_C cuprates, which have similar structures to the 1D cuprates such as $SrCuO_2$ or Sr_2CuO_3. In fact, the ARPES results on the quasi-2D copper oxides have similar broad peaks to the 1D cuprates.[10,11]

These low-dimensional electron systems are also known for strong nonlinear optical responses,[12,13] and they are expected to function as devices, such as optical switches. Therefore, it is important to clarify how the nature of quantum fluctuations changes with the interaction strength or doping in order to further understand the electronic structures in these materials.

In this research, quantum fluctuations in the 1D doped Hubbard model are clarified by using the resonating Hartree-Fock (res-HF) method.[14] So far, many sophisticated theories, such as the quantum Monte Carlo,[15] variational Monte Carlo,[16] and density-matrix renormalization group[17] methods, have been developed and applied to physics and chemistry. In addition, as far as the 1D Hubbard model is concerned, we have the exact solution.[18,19] However, this does not mean that we know everything about the 1D Hubbard system. Specifically, the nature of the quantum fluctuations in the doped systems remains an interesting yet controversial issue. Quantum fluctuations, which are intrinsic to interacting many-particle systems beyond the mean-field picture, are usually described by multiconfigurations, such as the path integration and configuration interactions. However, it has been quite difficult to obtain a physical picture on the quantum fluctuations from the conventional methods, though they have often reproduced the correlation structures or correlation energies very well. Thus, a direct description of the quantum fluctuations by the res-HF method would represent an important step toward a better understanding of the complicated physics in interacting many-particle systems. In the following sections, not only spin and charge behaviors but also general features of quantum fluctuations are clarified at different doping ratios and different interaction strengths.

The present paper is organized as follows. In Sec. II, the res-HF method is introduced, and we will show the reason

why this method is suitable for the direct description or visualization of the quantum fluctuations. In Sec. III, the method is applied to the 1D doped Hubbard model. Here, we will demonstrate how the nature of quantum fluctuations depends on the interaction strength and doping. A brief summary is given in Sec. IV.

II. METHOD

In the res-HF theory, a many-electron wave function is constructed by superposition of nonorthogonal Slater determinants (S-dets), such as

$$|\Psi\rangle = \sum_{n=1}^{N_S} C_n \sum_S P^S |\phi_n\rangle. \quad (1)$$

Here, N_S represents the number of constituting S-dets. The molecular orbitals of all the constituting S-dets $|\phi_n\rangle$, as well as their superposition coefficients C_n, are simultaneously optimized to minimize the res-HF energy $\langle\Psi|H|\Psi\rangle$. Nonorthogonal S-dets mutually incorporate the full electron excitation effects from other S-dets, and therefore, the res-HF wave function can describe large quantum fluctuations efficiently.[20,21] In this method, the different orbitals for different spin (DODS)-type S-dets are employed. The DODS-type S-det can describe the symmetry-broken state, such as the spin-density wave (SDW) or defects in the SDW, which play an important role in strongly correlated electron systems. On the other hand, the wave function itself should hold the original symmetries of the system. So far, it has been difficult to construct a reliable and symmetry-conserved many-electron wave function from the DODS-type S-dets. In the res-HF method, to recover these original symmetries, the symmetry projections are adopted for each S-det. For example, let us assume that the operator T makes a translation of the broken-symmetry S-det $|\phi\rangle$ by one site. Then, $T^m|\phi\rangle$ $(m=0,1,\ldots,N-1)$ are energetically degenerate. The set of $\{T^m|\phi\rangle\}$ is called a Goldstone set of $|\phi\rangle$. The original translation symmetry of the system is recovered by superposition of the Goldstone set.[22] In Eq. (1), P^S symbolically represents these spatial and spin symmetry projections.[23] Thus, we can construct the symmetry-conserved wave function with symmetry-broken S-dets. Here, when we say a res-HF wave function is constituted of N_S S-dets, we should note that symmetry projections are applied to each S-det. As a result, we superpose much more S-dets than N_S in actual calculations (for example, $N_S \times 1500$ S-dets for $N=50$ systems). The orbital optimization is carried out for N_S S-dets to minimize the expectation value of Hamiltonian, taking the symmetry projections into account. More details of the res-HF method are given in Ref. 24. The important feature of this method is that we can directly obtain a physical picture on the quantum fluctuations by analyzing the optimized S-dets. Furthermore, the res-HF method has no restriction on the band filling or dimensions. So far, this method has been successfully applied to largely deformed nuclei,[25] an *ab initio* calculation on a CO molecule,[21] and an interacting electron system.[24]

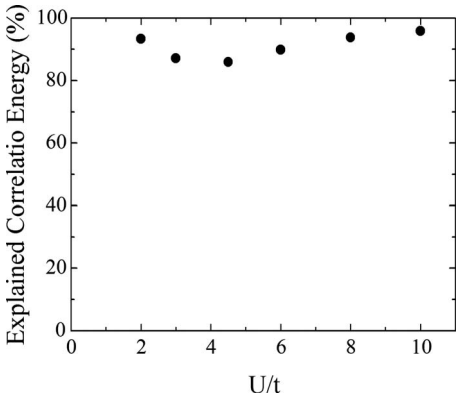

FIG. 1. U/t dependence of the correlation energy explained by the res-HF wave functions.

III. RESULTS AND DISCUSSION

Here, the res-HF method is applied to the 1D doped Hubbard model. Hamiltonian is given by

$$H = -t\sum_{l,\sigma}^{N} (a_{l,\sigma}^{\dagger} a_{l+1,\sigma} + a_{l+1,\sigma}^{\dagger} a_{l,\sigma}) + U\sum_{l}^{N} n_{l,\uparrow} n_{l,\downarrow}, \quad (2)$$

where N represents the system size. The number of electrons is denoted by N_e. Here, the periodic boundary condition is imposed, and therefore, the wave function is constructed to hold the D_N symmetry. In the following calculations, the res-HF wave functions are generated by $N_S=25$ S-dets.

First, to check the accuracy of the res-HF wave functions, their energies are compared with the exact Lieb-Wu solutions.[18,26] In Fig. 1, the ratio of the explained correlation energy is shown for $N=50$ and $N_e=46$, which is defined by

$$\kappa = \frac{E(\text{RHF}) - E(\text{res-HF})}{E(\text{RHF}) - E(\text{exact})} \times 100, \quad (3)$$

where E(RHF), E(exact), and E(res-HF) denote the energies of the restricted Hartree-Fock, exact, and res-HF solutions, respectively. In general, the correlation energy becomes largest in the intermediate interaction regime $(U/t \sim 4.5)$ since both quantum fluctuations in the weak and strong-interaction regimes coexist. In fact, as will be shown below, there exist quantum fluctuations due to Bloch-type states and spin-charge decoupled states in this interaction regime. Nevertheless, we can see that the res-HF wave functions explain more than 85% of the correlation energies in all the interaction regimes. The explained correlation energies are increased with the increase in N_S. As an example, in Fig. 2, N_S dependence of κ is shown for $U/t=4.5$. We have checked that further increase in N_S does not affect the physical pictures mentioned below, though it increases κ. Therefore, from these res-HF wave functions with $N_S=25$ S-dets, we can safely obtain reliable physical pictures on the quantum fluctuations in the doped Hubbard model.

In the previous paper, we showed that the spin projection significantly improves a res-HF wave function. In fact, the res-HF ground states are energetically lower than those obtained by the variational Monte Carlo method.[16,24] We have shown that not only the correlation energies but also the

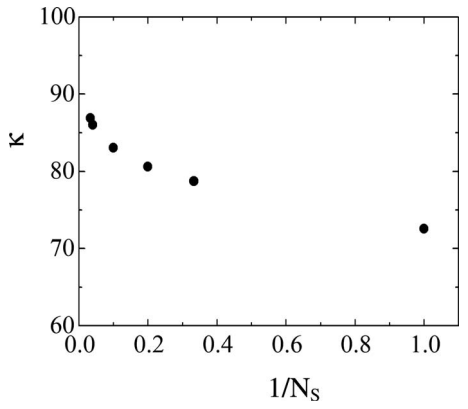

FIG. 2. N_S dependence of the correlation energy explained by the res-HF wave functions for $U/t=4.5$.

correlation structures are well described by the res-HF wave functions. On the other hand, the main purpose of the present research is to clarify quantum fluctuations in the doped Hubbard model systematically.

Now, we analyze the S-dets. The charge density (CD) and SD of the S-det ($|\phi\rangle$) at lth site are defined by

$$C_l = \langle\phi|a_{l\uparrow}^{\dagger}a_{l\uparrow} + a_{l\downarrow}^{\dagger}a_{l\downarrow}|\phi\rangle - 1.0,$$

$$S_l = \langle\phi|a_{l\uparrow}^{\dagger}a_{l\uparrow} - a_{l\downarrow}^{\dagger}a_{l\downarrow}|\phi\rangle, \tag{4}$$

respectively. The uniform SDW is represented by $C_l=0$ and $S_l=(-1)^{l-1}s'$, where s' denotes the amplitude of the SDW. We have an energetically degenerate SDW with the opposite phase, denoted by $C_l=0$ and $S_l=(-1)^l s'$. In the previous paper,[24] we showed that defects connecting these degenerate SDW's work as very important quantum fluctuations in the half-filled Hubbard model. In the doped case, as shown below, we have a significant modulation in the CD as well as the SD. To see this modulation in the CD (or SD), C_l (or S_l) is divided into its net and alternating components, NCD and ACD (or NSD and ASD), such as

$$C_l = \mathrm{NCD}(l) + (-1)^{(l-1)}\mathrm{ACD}(l),$$

$$S_l = \mathrm{NSD}(l) + (-1)^{(l-1)}\mathrm{ASD}(l). \tag{5}$$

The phase of the SDW changes where the ASD(l) changes its sign.

Here, we show U/t dependence of quantum fluctuations for $N=50$ and $N_e=46$ [$\delta=(N-N_e)/N=0.08$]. In Fig. 3, we show three typical S-dets, chosen from the res-HF wave functions for $U/t=3$(a), 6(b), and 10(c). In these figures, points where the ASD changes its sign, which means the SDW changes its phase, are denoted by black circles or black squares. Around a black circle, the NSD does not have a significant component, while we can see a large NCD component (its absolute value corresponds to a hole density). This topological defect in the SDW phase is usually called a holon. On the other hand, around a black square, we can see a large NSD component without a significant NCD component. This defect is called a spinon. In addition to these holons and spinons, we can see a spin-charge coupled defect denoted by a white circle. At a white circle, the ASD(l) touches the horizontal line of ASD=0, and both the NSD and NCD have significant components around it. This defect is called a polaron. Here, this polaron can be regarded as a bound state of a holon and a spinon. The orbital optimization for a res-HF state causes a little modification from the one-body orbitals. However, fortunately, this modification is not so large, and we can also use the above definitions for the holon, spinon, and polaron in the res-HF picture.

In the case of $U/t=3.0$(a), the S-det shown in Fig. 3 in the left panels (a-1) has holons and spinons, while the other two S-dets at the center (a-2) and right (a-3) panels have polarons as well as holons and spinons. The important feature in the weak-interaction regime is that all the S-dets have delocalized NCD components spreading over a whole system, as shown at the bottoms of (a-1), (a-2), and (a-3) in Fig. 3. Thus, our results indicate that not only the polarons and holons but also the Bloch-type states can be charge carriers in the weak-interaction regime. We should note that finite NCD components around black squares (spinons) mainly come from these delocalized Bloch-type states, polarons, and holons. The rest of $N_S=25$ S-dets have similar structures, having different numbers of holons, spinons, and polarons with different distances. Since these defects break translation symmetry, we superpose the Goldstone set[22] of each S-det, which have the same molecular orbitals as the original S-det but the positions of the defects are totally shifted site by site, as explained in Sec. II. Thus, from the above res-HF results, the quantum fluctuations in the weak-interaction regime can be described by the translation and breathing motions of holons, spinons, and polarons, with the background of the itinerant Bloch-type states.

In the case of $U/t=6$(b), on the other hand, we cannot see the delocalized NCD component as shown at the bottoms of (b-1), (b-2), and (b-3) in Fig. 3. The Bloch-type state disappears at about $U/t=5$. There still exist polarons in some S-dets as shown in the right panels (b-3), but the number of polarons is significantly decreased. These results clearly show that spin-charge separation is developing with the increase in the interaction strength.

In the case of $U/t=10$(c), the number of polarons is further decreased. Most of the S-dets contain only holons and spinons. The S-det shown in the right panels (c-3) includes the spin-charge coupled states, which are denoted by a gray circle and a gray square. It seems difficult to identify these states, but it is suggested that they would be a polaron splitting into a holonlike state (gray circle) and a spinonlike state (gray square), though they still have both spin and charge components. A spinon denoted by a black square is in between these decoupling states. Thus, polarons become unstable compared to holons and spinons in the strong-interaction regime. The rest of the S-dets have similar structures to these three S-dets. From the present results, we can conclude that the quantum fluctuations due to the translation and breathing motions of spinons and holons become

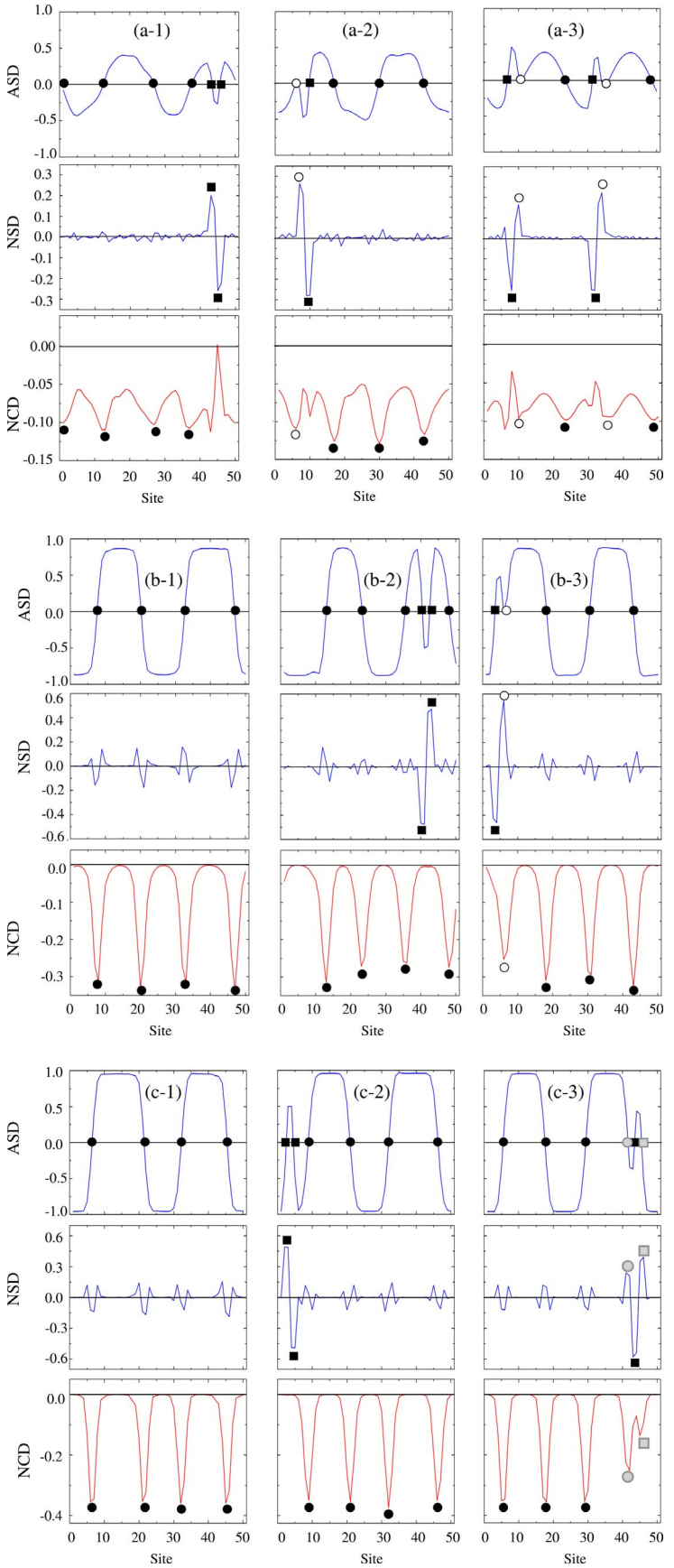

FIG. 3. (Color online) Structures of typical three of N_S=25 S-dets generating the res-HF wave functions for U/t=3(a), U/t=6(b), and U/t=10(c).

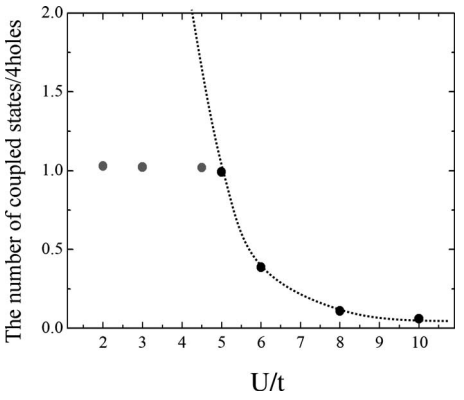

FIG. 4. U/t dependence of the number of spin-charge-coupled states for $N=50$ and $N_e=46$.

dominant in the strong-interaction regime, though the spin-charge coupled states still exist.

Figure 4 shows the U/t dependence of the number of polarons. In the res-HF method, the expectation value of this number $\langle N^c \rangle$ is obtained by

$$\langle N^c \rangle = \frac{\sum_{n=1}^{N_S} p_n N_n^c}{\sum_{n=1}^{N_S} p_n}, \tag{6}$$

where N_n^c is the number of polarons in the nth S-det. p_n denotes the probability to find the nth S-det in the res-HF wave function, which is given by

$$p_n = \langle \Psi | \sum_S P^S | \phi_n \rangle. \tag{7}$$

In Fig. 4, only the polaronlike states are taken into account, while the Bloch-type states are not included as it is complicated to estimate the number of the delocalized Bloch-type states. To make this point clear, the expectation values in the weak and intermediate interaction regimes ($U/t \leq 5$), where the S-dets have the Bloch-type states, are plotted by gray circles. Therefore, we should note that the actual number of the spin-charge coupled states including the Bloch-type states is larger than the values of the gray circles. The number of these Bloch-type states increases with the decrease in U/t. The rough behavior of the total number of the spin-charge coupled states is suggested by the dashed line. From Fig. 4, we can see that the number of polarons is very small in the strong-interaction regime, which indicates that the quantum fluctuations due to holons and spinons are dominant in this interaction regime. On the other hand, the number of polarons increases with the decrease in U/t. In addition, the Bloch-type states appear below $U/t=5$, and therefore, the quantum fluctuations due to these spin-charge coupled states also become important in the weak and intermediate interaction regimes.

In literature,[27] the energies of holons and polarons were compared in the framework of a projected Hartree-Fock (HF) approximation. In this method, a wave function is generated by a superposition of a Goldstone set of a single symmetry-broken S-det. They have concluded that holons are lower states than polarons in all the interaction regimes, and their energy difference increases with the increase in U/t. These results qualitatively agree with our res-HF results that polarons do not make dominant quantum fluctuations in all the interaction regimes, and the number of polarons decreases with the increase in U/t. In the res-HF method, multiple independent S-dets are employed and their orbitals are optimized with taking symmetry projections into account. Therefore, the res-HF method goes beyond the projected HF approximation. Or, we can say that the res-HF method is a natural extension of the projected HF approximation. We have shown that the res-HF wave functions contain both holons and polarons. It indicates that resonance or quantum interference among these states lowers the many-body ground state. A single S-det cannot explain such a resonance of different states. Quantum fluctuations due to polarons are not negligible especially in the weak and intermediate interaction regimes.

Here, we discuss the ARPES experiments. In the ARPES on $SrCuO_2$, they have concluded that two branches corresponding to holons and spinons are observed.[3] However, the ARPES data seem to have a more complicated aspect of the strongly correlated electron systems. As aforementioned, the ARPES data on the 1D correlated materials have broad peaks of the order of 1 eV, which indicate the importance of the incoherent component originating from the spin-charge coupling. These results are natural since the spin-charge separation is complete only in the strong-interaction limit. Real materials do not usually lie in such an extreme limit. In the experiment, all we know is a response on a perturbation added to the system. We cannot directly see the ground state itself. The ARPES also reflects the dynamical nature of interacting electrons. As a result, the ARPES data inevitably incorporate the incoherent components due to the scattering of a photoelectron (or a photocreated hole left in the solid) and elementary excitations, in addition to the coherent band component. This is not a drawback of the ARPES but is a merit to understand the many-body effects. On the other hand, so far, we have clarified the static quantum fluctuations in the realistic interaction regimes. By connecting these static fluctuations to the responses of perturbations, the understanding of the strongly correlated electron systems will become deeper. Our results have shown that quantum fluctuations due to holons and spinons are dominant in all the interaction regimes. These holons and spinons will make different branches in the ARPES peaks. However, at the same time, we have small but finite quantum fluctuations due to spin-charge coupled states. This intrinsic spin-charge coupling is important when we consider the responses on the external perturbations. For example, the perturbation on the charge degree of freedom can induce the spin excitations via the spin-charge coupled states. Since the 1D correlated materials have low energy magnetic excitations near $k=0$, finite spin-charge coupling causes the multiple magnetic excitations accompanied by the photoemission of an electron. In fact, the author previously showed that a broad ARPES peak is dominated by these many-body effects due to the spin-charge coupling.[6] Thus, we can comprehensively understand

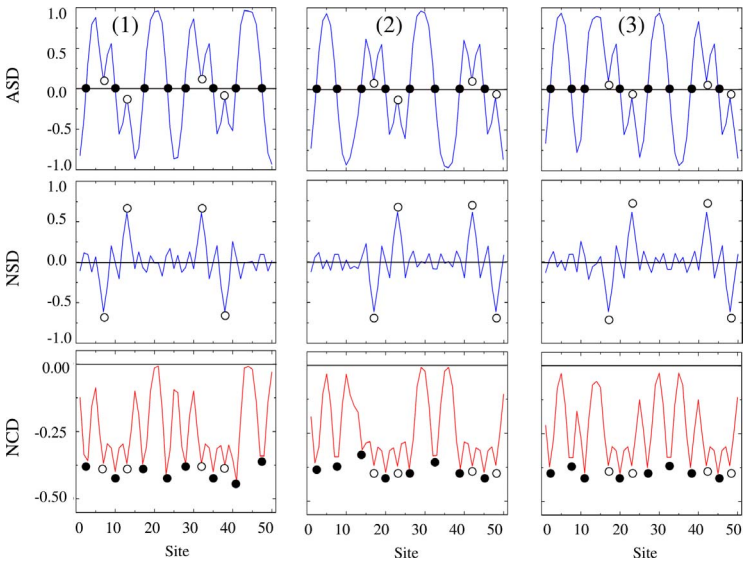

FIG. 5. (Color online) Structures of three typical S-dets generating the res-HF wave function for $U/t=10$ and $N_e=38$.

how spin-charge separation and coupling work in the ARPES data of the 1D electron systems by connecting the present results to the experiments.

Next, to see the doping dependence of quantum fluctuations, we show in Fig. 5 the structures of three typical S-dets for $N=50$ and $N_e=38(\delta=0.24)$ at $U/t=10$. In the strong-interaction regime with $N_e=46(\delta=0.08)$, the quantum fluctuations due to holons and spinons are dominant, as shown in Fig. 3(c). On the other hand, from Fig. 5, we can see many polarons as well as holons. The rest of the S-dets have the similar structures. Therefore, we can say that the number of the spin-charge coupled states increases with the increase in the doping.

When we further increase the doping, the nature of quantum fluctuations changes drastically. The concepts of holons, spinons, and polarons in the SDW do not work anymore. In Fig. 6, we show the spin and charge densities of two different

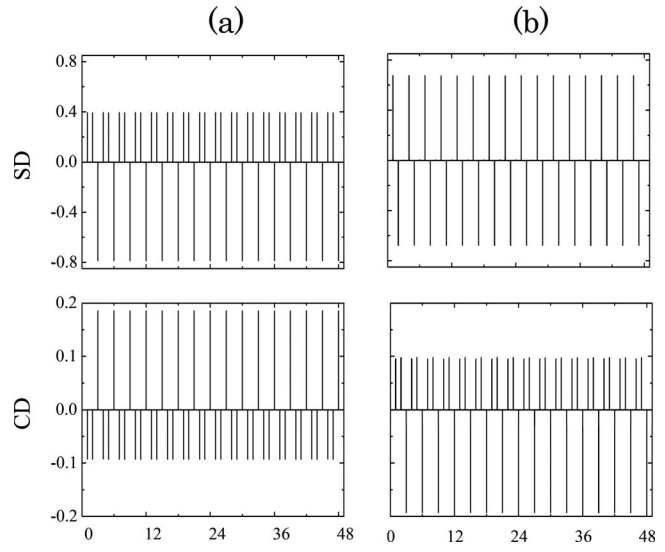

FIG. 6. Two different HF states referred to as A (a) and B (b) in the text for $U/t=6$, $N=48$, and $N_e=32$.

HF states for $N=48$, $N_e=32(\delta=1/3)$, and $U/t=6$. Their spin structures are described by $(\uparrow,\uparrow,\downarrow,\uparrow,\uparrow,\downarrow,\ldots)$ (a) (hereafter referred to as state A) and $(\uparrow,\downarrow,\cdot,\uparrow,\downarrow,\cdot,\ldots)$ (b) (hereafter referred to as state B). Both states have triple periodicity to the lattice, which comes from the nesting of the Fermi surface in the 1/3-filled electron systems. In the HF approximation, state A has a lower energy than state B in all the interaction regimes. We have also checked that the projected HF approximation does not change their energy relation. State A has a lower energy than B even after the symmetry projections. On the other hand, the res-HF wave function shows that the many-body ground state is qualitatively described by mixtures of these two states. In Fig. 7, three typical S-dets generating the res-HF wave function are shown, where all the parameters are the same as in Fig. 6. From Fig. 7, we can see that the dominant electronic structure is close to state B. Figures 7(a) and 7(b) show that small domains of state A are inserted (circles), while Fig. 7(c) shows another defect which simply reduces the amplitude of the spin density. The rest of the S-dets have similar structures to these three S-dets given in Fig. 7. Such a reverse in the energy relation sometimes occurs in strongly correlated electron systems. A famous example is that the bond alternation in the 1D system is stabilized by the on-site Coulomb repulsion, which is contrary to the HF picture.[28] In the present case, the res-HF wave function shows that the B-type ground state is stabilized by the translation and breathing motions of small domains of state A, as well as those motions of defects reducing the spin density, due to their resonance. This is an interesting many-body effect beyond the (projected) HF approximation, and the res-HF method gives a physical picture on this many-body effect through the quantum fluctuations.

IV. SUMMARY

We have succeeded to visualize the quantum fluctuations in the 1D doped Hubbard model. Especially, the spin-charge behaviors have been consistently explained from the strong to the weak-interaction regimes. In the case of $\delta=0.08$, the

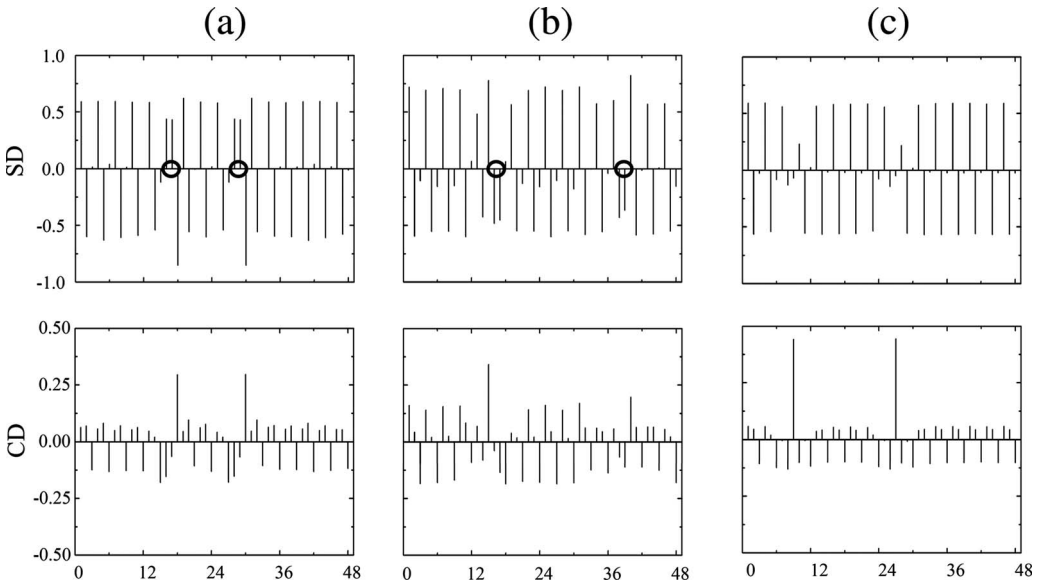

FIG. 7. Structures of three typical S-dets generating the res-HF wave function for $U/t=6$, $N=48$, and $N_e=32$.

quantum fluctuations are described mainly as the translation and breathing motions of holons and spinons in the strong-interaction regime, while those due to polaron as well as holons and spinons are important in the weak and intermediate interaction regimes. In the case of $\delta=0.24$, the quantum fluctuations due to polarons become important even in the strong-interaction regime. In the case of $\delta=1/3$, we have shown that the concepts of holons, spinons, and polarons do not work anymore. The many-body ground state has state B-type electron structure with quantum fluctuations due to domains of state A.

ACKNOWLEDGMENTS

This work was supported by Grant-in-Aid for Scientific Research No. 18540327 and the Next Super Computing Project, Nanoscience Program, MEXT, Japan.

[1] M. Ogata and H. Shiba, Phys. Rev. B **41**, 2326 (1990).
[2] J. Voit, Phys. Rev. B **47**, 6740 (1993).
[3] B. J. Kim, H. Koh, E. Rotenberg, S.-J. Oh, H. Eisaki, N. Motoyama, S. Uchida, T. Tohoyama, S. Maekawa, Z. X. Shen, and C. Kim, Nat. Phys. **2**, 397 (2006).
[4] S. Suga, A. Shigemoto, A. Sekiyama, S. Imada, A. Yamasaki, A. Irizawa, S. Kasai, Y. Saitoh, T. Muro, N. Tomita, K. Nasu, H. Eisaki, and Y. Ueda, Phys. Rev. B **70**, 155106 (2004).
[5] S. I. Fujimori, A. Ino, T. Okane, A. Fujimori, K. Okada, T. Manabe, M. Yamashita, H. Kishida, and H. Okamoto, Phys. Rev. Lett. **88**, 247601 (2002).
[6] N. Tomita and K. Nasu, Phys. Rev. B **60**, 8602 (1999).
[7] P. W. Anderson, Science **235**, 1196 (1987).
[8] A. Kampf and J. R. Schrieffer, Phys. Rev. B **41**, 6399 (1990).
[9] T. Moriya, Y. Takahashi, and K. Ueda, J. Phys. Soc. Jpn. **59**, 2905 (1990).
[10] J. J. M. Pothuizen, R. Eder, N. T. Hien, M. Matoba, A. A. Menovsky, and G. A. Sawatzky, Phys. Rev. Lett. **78**, 717 (1997).
[11] K. M. Shen, F. Ronning, D. H. Lu, W. S. Lee, N. J. C. Ingle, W. Meevasana, F. Baumberger, A. D. Damascelli, N. P. Armitage, L. L. Miller, Y. Kohsaka, M. Azuma, M. Takano, H. Takagi, and Z. X. Shen, Phys. Rev. Lett. **93**, 267002 (2004).
[12] H. Kishida, H. Matsuzaki, H. Okamoto, T. Manabe, M. Yamashita, Y. Taguchi, and Y. Tokura, Nature (London) **405**, 929 (2000).
[13] S. Iwai, M. Ono, A. Maeda, H. Matsuzaki, H. Kishida, H. Okamoto, and Y. Tokura, Phys. Rev. Lett. **91**, 057401 (2003).
[14] H. Fukutome, Prog. Theor. Phys. **80**, 417 (1988).
[15] *Quantum Monte Carlo Method in Condensed Matter Physics*, edited by M. Suzuki (World Scientific, Singapore, 1993).
[16] H. Yokoyama and H. Shiba, J. Phys. Soc. Jpn. **56**, 3582 (1987).
[17] S. R. White, Phys. Rev. Lett. **69**, 2863 (1992).
[18] E. H. Lieb and F. Y. Wu, Phys. Rev. Lett. **20**, 1445 (1968).
[19] N. Kawakami and S.-K. Yang, Phys. Lett. A **148**, 359 (1990).
[20] H. Koch and E. Dalgaard, Chem. Phys. Lett. **212**, 193 (1993).
[21] N. Tomita, S. Ten-no, and Y. Tanimura, Chem. Phys. Lett. **263**, 687 (1996).
[22] R. E. Peierls and J. Yoccoz, Proc. Phys. Soc., London Sect. A **70**, 381 (1957).
[23] A. Igawa, Int. J. Quantum Chem. **54**, 235 (1995).
[24] N. Tomita, Phys. Rev. B **69**, 045110 (2004).
[25] S. Nishiyama, Nucl. Phys. A **576**, 317 (1994).
[26] K. Hashimoto, Int. J. Quantum Chem. **30**, 633 (1986).
[27] M. Berciu and S. John, Phys. Rev. B **61**, 10015 (2000).
[28] J. E. Hirsch, Phys. Rev. Lett. **51**, 296 (1983).